Long-Term Stability of 1-cm Thick Pixelated HgI_2 Gamma-Ray Spectrometers Operating at Room Temperature

James E. Baciak, *Student Member, IEEE* and Zhong He, *Senior Member, IEEE*

***Abstract*—Thick mercuric iodide (HgI_2) detectors are being investigated as potential room temperature gamma-ray spectrometers. This paper presents an investigation of the polarization effects and long-term spectral stability of pixelated HgI_2. Pixelated HgI_2 detectors have shown good stability over several months of measurements. After the first four days, the photopeak position and resolution have remained relatively constant. Current pixelated HgI_2 detectors may not suffer from polarization effects that once severely limited past planar HgI_2 devices, and can have good energy resolution (approximately 2% for a Cs-137 source) while using a modest electric field (~2500 V/cm) and a relatively short shaping time (8 μs).**

I. Introduction

FOR MANY years, mercuric iodide (HgI_2) has been studied as a semiconductor detector medium for room temperature gamma-ray spectroscopy [1]–[3]. HgI_2 has many attributes that make the material an ideal gamma-ray spectrometer. The high atomic numbers of HgI_2 (80 and 53) make for a relatively large photoelectric cross section for gamma-ray interactions when compared with other gamma-ray spectroscopy materials (such as Ge, NaI, and CdZnTe). HgI_2 has relatively high gamma-ray stopping power due to the high density (6.4 g/cm^3) of the material. The wide band-gap of the material (2.13 eV) allows for room temperature (or higher) operation without excessive noise from thermal leakage current.

However, like many compound semiconductor materials proposed as room temperature semiconductor radiation detectors, HgI_2 suffers from poor charge carrier mobility particularly for holes that are severely trapped. HgI_2 detectors also suffer from material nonuniformity. Due to these effects, the charge induced on the electrodes depends on the position of the radiation interaction. Thus, HgI_2 detectors have generally been limited to only a few mm in thickness using a large electric field when operated as a spectrometer in order to keep the effect of incomplete charge collection and interaction depth dependence on the electrode signals to a minimum. Pulse processing techniques [4] have shown some improvement in reducing the effects of the depth-dependent signal, but these techniques cannot overcome the poor signal-to-noise ratio produced for a large fraction of the detector volume.

In order to increase the HgI_2 detector thickness while also improving the spectroscopic performance of the detectors, the depth dependence of the pulse generated by a gamma-ray interaction must be reduced. Single polarity charge sensing is one technique that can overcome the severe hole trapping present in wide band-gap semiconductor detectors. A design used in single polarity charge sensing is pixelated anodes [5]. Pixelated detectors have shown improved energy resolution over detectors with conventional planar electrodes [6]. The use of depth sensing and depth correction of the anode pixel signal has been shown to improve the resolution of gamma-ray spectra from pixelated HgI_2 detectors [7].

Another problem associated with several compound semiconductor materials in the past is polarization, which has limited the use of many wide room-temperature detector materials, including CdTe [8] and HgI_2 [9], [10]. Polarization can be due to the migration of impurities while the detector is biased. This can cause a change of the spectral response of the detector over a period of time. In this paper, we present results from a study over several months of the spectral response of pixelated HgI_2 detectors currently being proposed as a gamma-ray spectrometer that can operate at room temperature. The photopeak resolution, position, and count rate are analyzed as functions of time.

II. Detector Design and Setup

Fig. 1 shows the new pixelated anode configuration designed for the current 1-cm^3 HgI_2 detectors used in this work. Similar to the previous design [11], the detector has four pixels each with an area of 1 mm^2. However, the new design placed all four pixels next to each other in the central area of the detector. The pixels were surrounded on the outside by a large anode. All electrodes were made of palladium and were deposited on the detector by sputtering. The total cross-sectional area of the detector was approximately 1 cm^2.

A negative potential was applied to the planar cathode. Thus, the electrons will move toward the anode side of the detector. When the gamma-ray interacts in the detector material underneath a pixel, the induced charge on the pixel is mainly determined by the number of electrons collected by the pixel and only slightly dependent on the interaction depth. The pixel signal is not significantly affected by hole movement, and any interaction in the volume outside the pixel region does not induce a charge

Manuscript received October 19, 2003; revised May 14, 2004.

This work was supported in part by Constellation Technology Corporation, Largo, FL 33777 USA.

J. E. Baciak is with the Department of Nuclear and Radiological Engineering, University of Florida, Gainesville, FL 32611 USA (e-mail: jimmer@ufl.edu).

Z. He is with the Department of Nuclear Engineering and Radiological Sciences, University of Michigan, Ann Arbor, MI 48109 USA (e-mail: hezhong@umich.edu).

Digital Object Identifier 10.1109/TNS.2004.832900

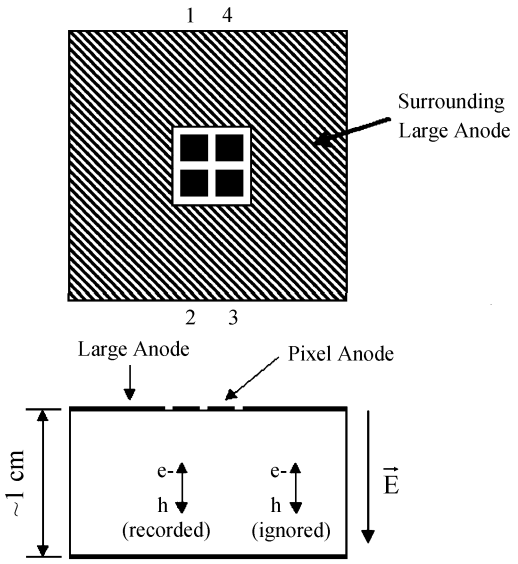

Fig. 1. HgI_2 detector crystal setup. Top: top view of anode electrode configuration. The four pixels are now adjacent to each other, as opposed to the previous design. Bottom: cross-sectional side view. Only events under each pixel are recorded by the anode pixel and events underneath the noncollecting large anode are ignored. Note that pixel #3 was not analyzed due to a poor output signal.

on the pixel of interest. The signal on the planar cathode is determined by both electron and hole movement. However, the holes have poor mobility and are severely trapped, and thus do not contribute a significant signal to the cathode. Thus, the cathode signal is monotonically dependent on the interaction depth. A gamma-ray interaction near the cathode will induced a much larger signal on the cathode than an interaction near the anode of the same energy. By calculating the cathode to anode pixel signal ratio (C/A), the interaction depth can be determined [12].

In addition to the negative bias applied to the cathode, each anode electrode (including the large surrounding anode) is grounded to the detector box through an AmpTek A250 charge sensitive amplifier [13] by utilizing the bias supply circuit on the preamplifier board. When performing gamma-ray spectroscopy measurements, one anode pixel and the cathode signal are connected to standard NIM shaping amplifiers. The shaped pulses were connected to peak-hold circuitry to hold the peak of the shaped pulse prior to the ADC sampling the pulse amplitude. The peak-hold circuit eliminates any change in signal amplitude due to differences in the peaking times of the cathode and anode pixel signals. The ADC card used in this study was a National Instruments [14] PCI card. The spectra were generated using LabView™ and analyzed using Matlab®. The HgI_2 detector was irradiated from the cathode side using point sources.

III. Pulse Waveforms From a 1-cm Thick HgI_2 Detector

Example pulse waveforms from the different electrodes for a single gamma-ray interaction are shown in Fig. 2. The pulse heights of the cathode and anode pixel were nearly equal. Since the cathode signal has a linear dependence on the depth of interaction, the nearly equal induced charge on both the cathode and anode pixel indicates that this gamma-ray interaction occurred near the cathode. The linear increase of the pulse from

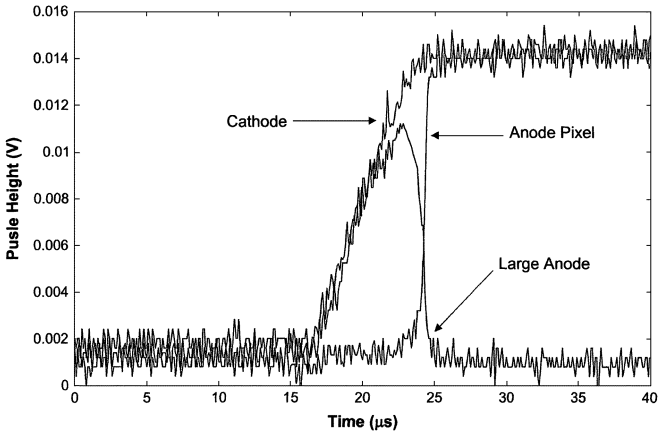

Fig. 2. Pulse waveforms for the planar cathode, large anode, and anode pixel for a single interaction gamma-ray event. Based on the pulse height of the cathode signal, the event took place relatively near the cathode side of the detector.

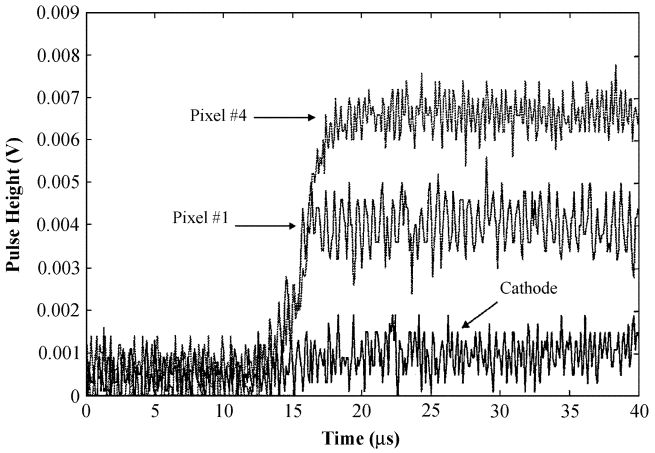

Fig. 3. Pulse waveforms showing charge sharing between two pixels. Here, electrons are collected on two adjacent pixel from the same gamma-ray interaction. The absence of a significant pulse on the cathode suggests the interaction occurred near the anode side of the detector.

the planar cathode can clearly be seen, while the pulse generated on the anode pixel increases rapidly only when the electrons move near the pixel (within one pitch depth). The large surrounding anode signal behaves similarly to the planar cathode as the signal rises, then its signal drops rapidly once the electrons approach the pixel. At that point the electrons are being collected by the anode pixel and the large anode (which does not collect electrons in this case) signal will return to its baseline. The new baseline of the large anode signal after the electrons were collected is slightly negative with respect to the original baseline (less than 0.5-mV difference). The large anode signals are highly dependent on the depth of interaction (similar to the cathode), and this slightly negative baseline indicates that the event occurred within the detector, but very close to the cathode side whereby the cathode signal is not significantly affected. An adjacent pixel will also increase slightly, but fall back to the original baseline once the electrons are collected by another anode electrode.

Since the pixels have been placed next to each other, and the large surrounding anode has been connected, the effects of charge sharing can be observed. Fig. 3 shows charge sharing be-

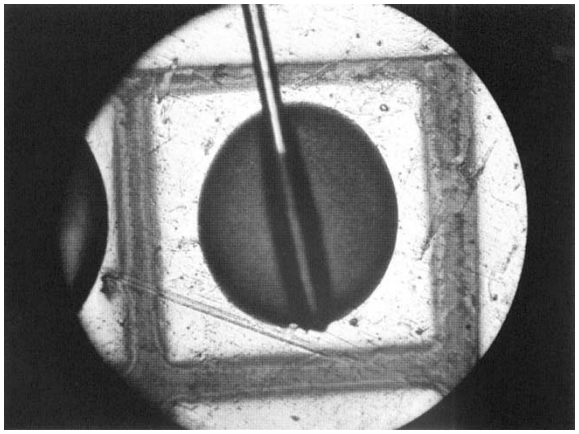

Fig. 4. Photograph of a normal pixel. In this case, the gap between the electrodes is clearly defined on all four sides.

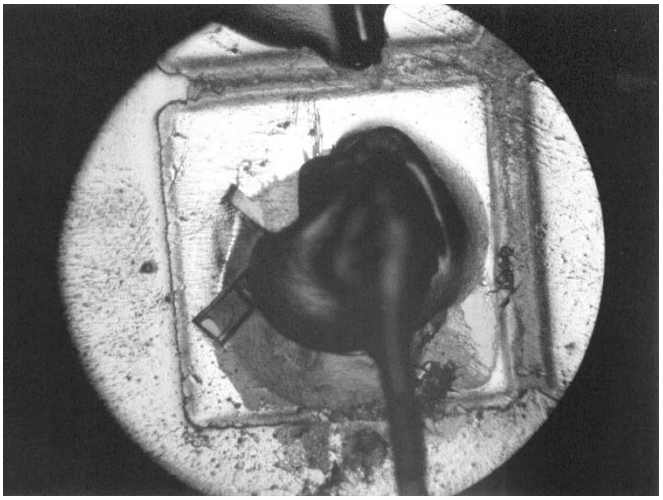

Fig. 5. Photograph of a pixel where the surrounding large anode is in direct contact with the pixel. This pixel will therefore behave like the large anode and be unable to produce a well resolved photopeak.

tween pixels. Two pixel pulses rise nearly simultaneously with approximately 60% of the charge collected on pixel #4 and 40% collected on pixel #1 (see Fig. 1 for the pixel layout). The absence of a significant pulse on the planar cathode indicates that the gamma-ray interaction took place near the anode side of the detector. For this work, only one pixel is measured during the spectra collection time. Thus, events that undergo multiple pixel interactions cannot be combined to improve the photopeak efficiency of the detectors. In future work, it would be ideal to be able to generate spectra from multiple pixel interactions.

It should be noted that one of the pixels (pixel #3) on the detector used in this work did not work. In fact, several detectors with the new electrode design suffered from having pixels electrically connected to the large anode. Fig. 4 shows a normal working pixel. The pixel clearly has a surrounding gap region that separates the pixel from the adjacent electrodes. However, Fig. 5 shows a pixel in direct electrical contact with the surrounding large anode. This pixel will behave exactly like the large anode (severe depth dependence of the signal). The remaining three pixels were in good working order and spectra were obtained using these pixels. The electrode deposition process needs to be improved before designing a fully pixelated detector.

IV. Spectroscopic Performance of Pixelated HgI_2

Fig. 6 shows a typical spectrum obtained from the 1-cm^3 HgI_2 detector. While the resolution of the spectrum was near 3% at 662 keV ($\sim$20 keV), the resolution was improved by incorporating depth sensing and correction into the spectra. Depth sensing also allows for the generation of spectra from the anode pixel signal (Fig. 7) according to the depth index determined by the C/A ratio. The spectrum in Fig. 6 was divided into approximately 18 depth indices (larger valued depth indices correspond to events closer to the cathode). Thus, analysis of resolution and peak counts as a function of depth was performed (Fig. 8). Fig. 7 shows that a photopeak can be observed for nearly the entire thickness of the detector (near anode events, i.e., depth index 1, will suffer from severe depth dependence on the induced signal). The depth corrected energy resolutions for pixels #1, #2, and #4 were 2.3%, 2.6%, and 1.8%, respectively. These spectra were

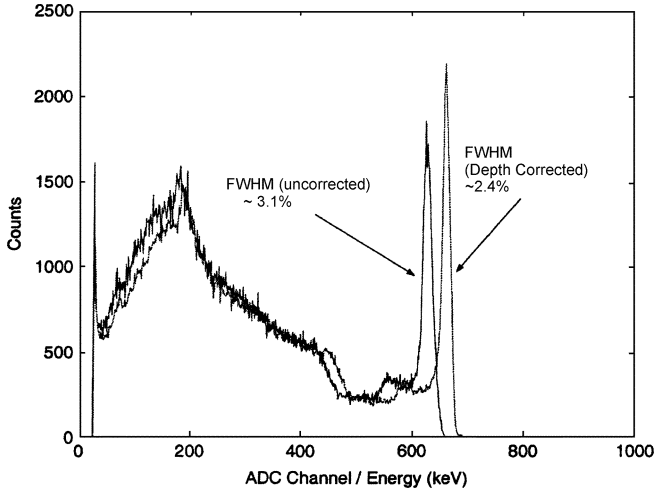

Fig. 6. Cs-137 spectrum from Det. 93203N98, pixel #1 at a bias of 2500 V and using a shaping time of 8 μs. The incorporation of depth sensing and correction improved the 662-keV photopeak resolution from 3.1% FWHM to 2.4% FWHM. The resolution of the detectors with the new electrode layout was worse than expected due to the wide gap between the anode pixel and the large surrounding anode.

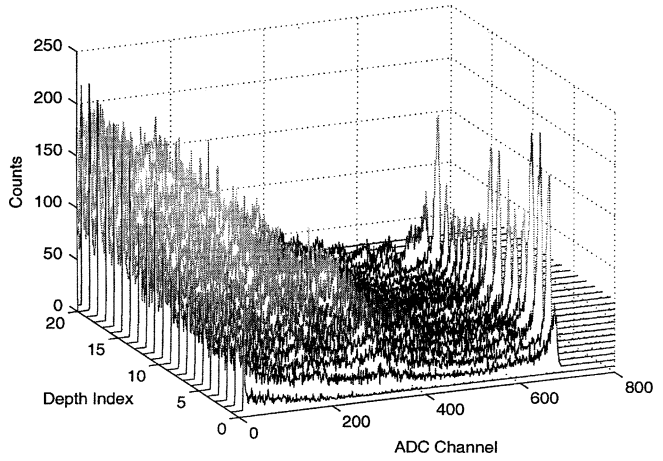

Fig. 7. Using depth sensing, a plot of the anode pixel spectra as a function of the interaction depth can be constructed. Here, the spectra of Det. 93203N98 pixel #4 are shown for entire thickness of the detector.

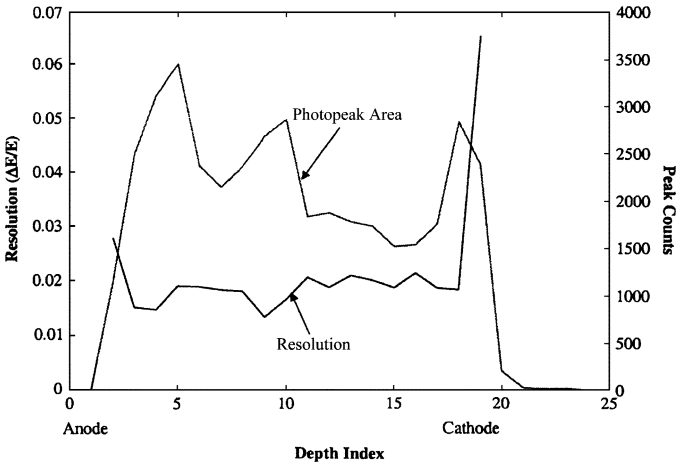

Fig. 8. Resolution and peak count as a function of depth are shown together. The resolution degraded slightly near the cathode side of the detector due to increased charge trapping and sharing between anode electrodes. The large photopeak area in the middle of the detector and near the anode side suggest that the volume of each depth index is not constant.

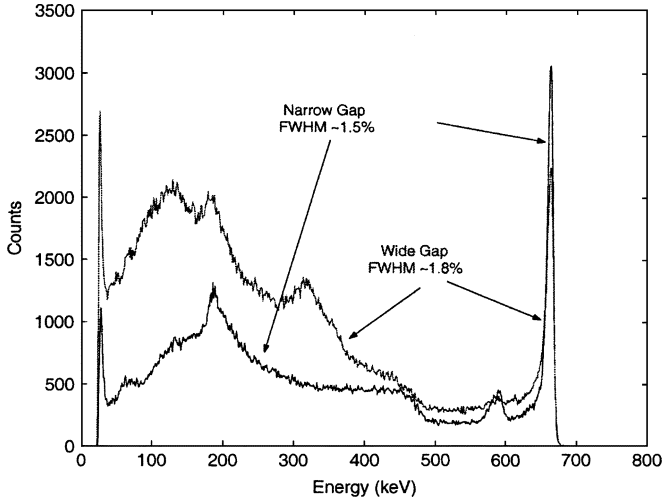

Fig. 9. Comparison of depth corrected Cs-137 spectra between the new and old electrode layout reveals that the number of events in the continuum dramatically increased due to excess charge sharing from gamma-ray events in the large gap between the pixel and surrounding electrode. Increased charge sharing may have also degraded the photopeak resolution by increasing the low-energy tail of the peak.

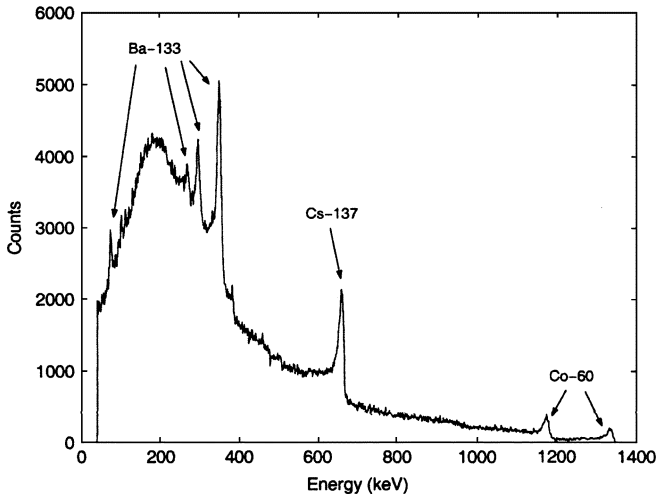

Fig. 10. Depth corrected spectra for a mixed source spectra. In this case, three sources (Ba-133, Cs-137, and Co-60) were placed under the cathode and a one-day spectrum was collected for Det. 93203N98, pixel #4. The resolution of the 1332-keV gamma-ray from Co-60 was approximately 1.7%.

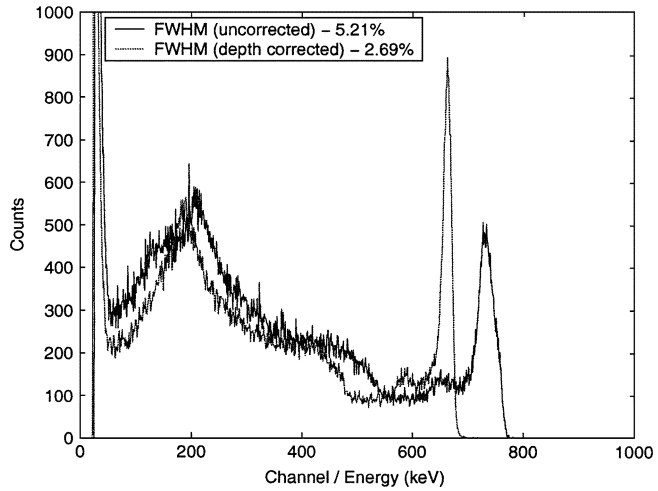

Fig. 11. Cs-137 spectrum for first 8 hours after biasing the detector to −2500 V. The shaping time used in the long-term stability measurements was 8 μs. Depth correction improved the resolution of the photopeak from 5.3% to 2.7%.

collected with a relatively low electric field for HgI_2 detectors (2500 V/cm) and modest shaping times (4–16 μs).

Resolution as a function of interaction position can be measured with pixelated room-temperature semiconductor detectors [15]. Fig. 8 shows that the resolution as a function of depth remains relatively constant, but will degrade slightly toward the cathode side due to an increase in charge trapping and sharing between electrodes. Hole movement may have been the cause of the increased photopeak area near the both electrodes, and the increased area around depth index 9 may be due to some nonlinear effects of the weighting potential. The photopeak area near the cathode was expected to be higher since the detector was irradiated from under the cathode. The increase in peak area closer to the anode side of the detector was due to charge diffusion and sharing between electrodes. Charge sharing due to diffusion is increased for events that take place closer to the cathode, as electrons must travel a greater distance. Events that occur near the peripheral region of the pixel will have a reduced induced charge on the pixel as electrons are lost to the gap region or collected by another anode electrode. Thus the C/A ratio measurement will affect the value of the calculated depth index, including increasing the value beyond depth index 18 (the near cathode events). Charge trapping and charge sharing will reduce the effective volume of the detector crystal near the cathode that physically contributes to the photopeak. Therefore, the effective volume of the pixel region near the anode may be larger than that near the cathode and the photopeak area near the anode side of the detector can be higher.

Comparing the spectra with a typical spectra from an older detector with the anode pixels separated from each other, one notices that the number of counts in the Compton continuum region in the new detector is significantly larger in the new design (Fig. 9) [9]. This can be explained by the gap region. The design specifications for the detector called for a gap region of

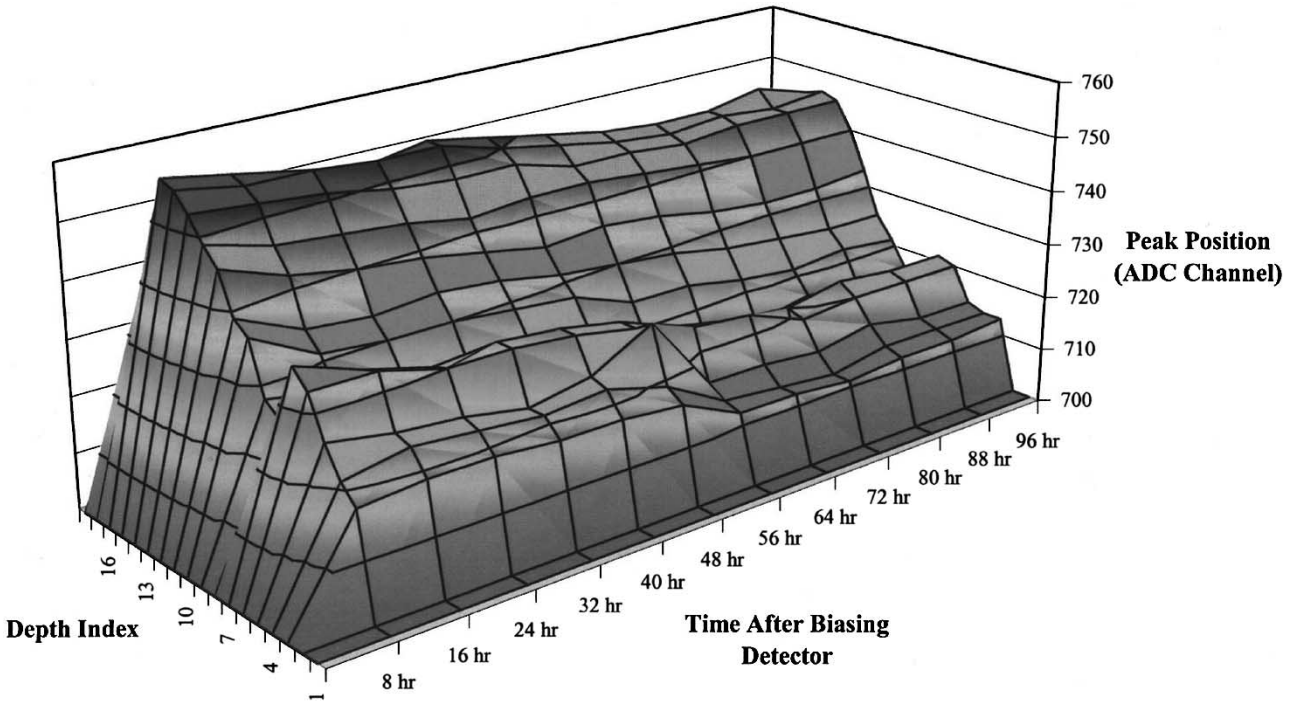

Fig. 12. Photopeak position as a function of both depth index and time after biasing the detector. There is a slightly larger decrease in the photopeak position for events near the cathode as opposed to near anode events.

approximately 150 μm, the same gap dimension as the previous electrode design. Due to electrode deposition difficulties, the gap between the pixels and surrounding anode on the new design was actually 500 μm. Gamma-ray interactions in the gap region will share charge between the pixels and large anode and an increased gap region will increase charge sharing. Despite this production flaw, the performance of the detector was better than what could be expected from a 1-cm^3 HgI_2 detector with conventional planar electrodes.

In addition to the single photopeak gamma-ray spectra, spectra with multiple lines were also obtained. A depth corrected spectrum from a collection of sources (Ba-133, Co-60, and Cs-137) is shown in Fig. 10. The five gamma-ray energies of Ba-133 and the Cs-137 peak can clearly be seen. However, the two photopeaks from Co-60 are difficult to observe due to the low activity of the source used in the experment ($\sim$2 μCi) compared to the other sources ($\sim$10 μCi). If the lower activity and lower detection efficiency of the higher energy gamma-rays are accounted for, the relative peak areas are consistent within the error of the source activities, which was approximately 10%.

V. Polarization of Pixelated HgI_2 Detectors

An eight hour spectrum was collected immediately after applying a cathode bias of -2500 V (Fig. 11). The depth corrected spectrum had a resolution of approximately 2.7% at 622 keV. The resolution was worse than expected, but this may have been due to the presence of a large gap between the pixel and the large surrounding anode that will contribute an increase in charge sharing and trapping between the two electrodes.

In addition to the depth corrected spectra shown above, depth and time dependent data were collected from the pixels. Fig. 12 shows the photopeak position as a function of both depth index and time for the first 4 days after biasing the detector. Fig. 12 shows that the photopeak position decreases slightly with time (approximately 1–2%) across all depths of the detector, but decreases slightly more near the cathode side of the detector. A slight shift in the photopeak position can be seen in Fig. 13, which shows three Cs-137 spectra. There is the slight shift between hours 8 and 80, but the photo peaks 80 h and 160 h after biasing the detector were nearly identical.

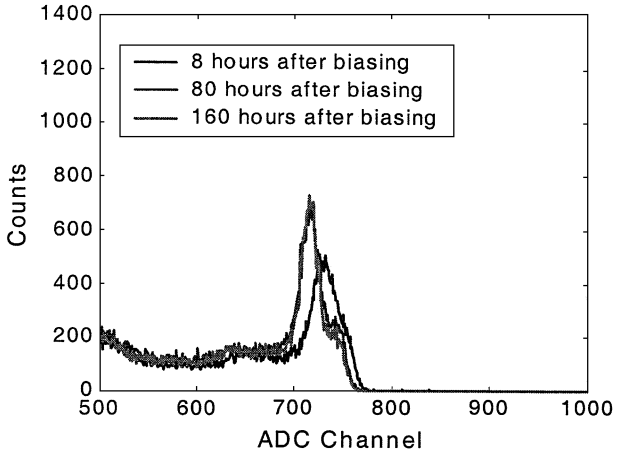

Fig. 13. Cs-137 anode pixel spectra (zoomed to show the photopeak) at three different time periods after biasing the HgI_2 detector. Each measurement was eight hours in duration. After the first three days after biasing the detector, there was very little change in the photopeak characteristics (peak area, resolution, and position.

Fig. 14 shows that the resolution as a function of depth and time remained relatively consistent during the first four days of measurements. However, one measurement (56 h after biasing) showed a worse resolution and may have been due to increased

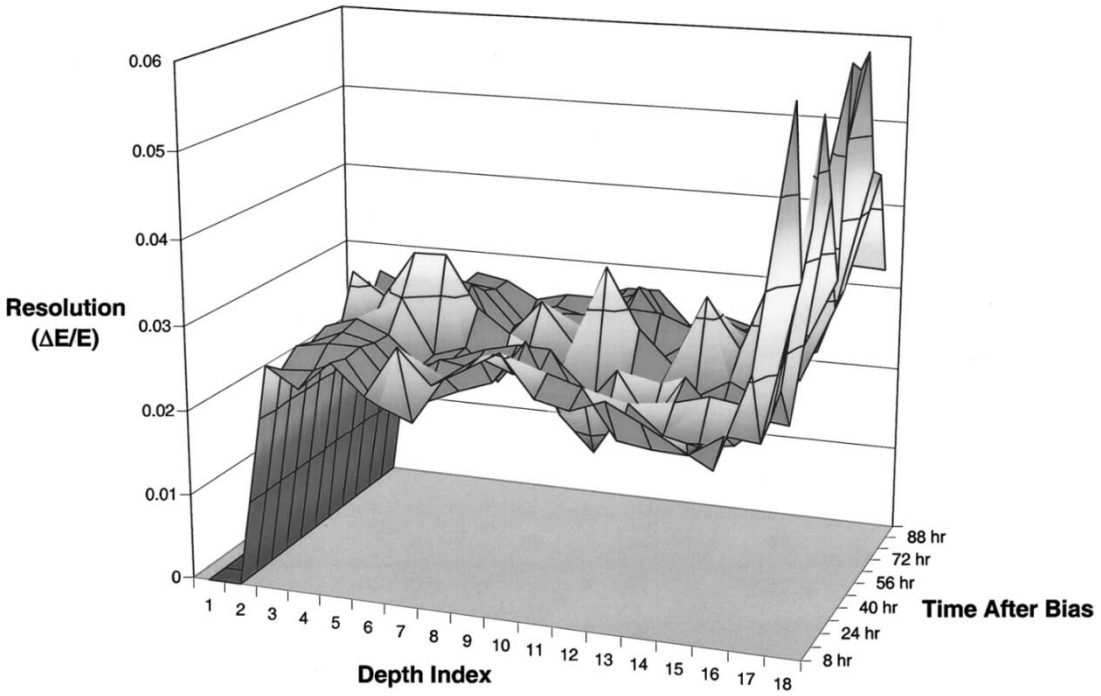

Fig. 14. Photopeak resolution as a function of depth and time. The peak resolution remained relatively consistent with the exception of the measurement 56 h after biasing the detector.

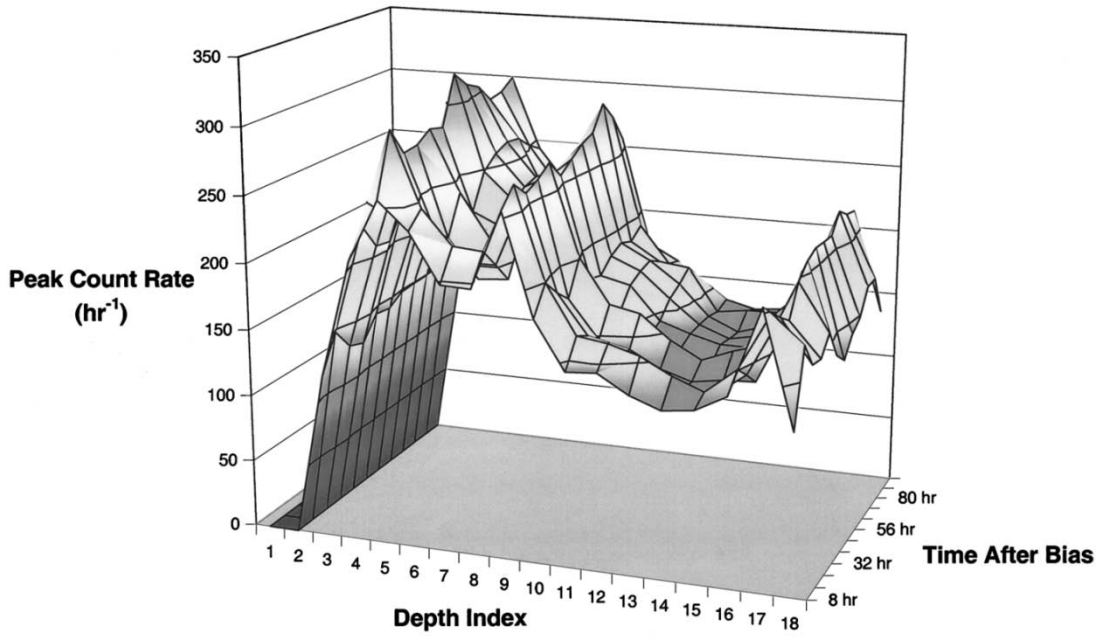

Fig. 15. The photopeak count rate remained relatively constant with respect to the position of interaction and time. The large number of events near the anode and for depth index 8 suggest that the effective volume of the pixel changes as a function of depth. The small peak in counts near the cathode was due to some hole movement in the detector crystal.

noise during that time. It is unclear what may have caused the increased noise at that time frame, but this effect was not observed again during the remainder of the measurement period (about 120 days). Fig. 14 also shows a much worse resolution for photopeak events that had a large C/A ratio. When more electron trapping or charge sharing occurs, the anode pixel signal is reduced which increases the C/A ratio. This suggests that the effects of charge trapping and charge sharing between anode electrodes degraded the resolution.

The photopeak count rate as a function of depth and time, as seen in Fig. 15, are relatively constant during the first 4 days, suggesting that the effective volume of the pixel remained

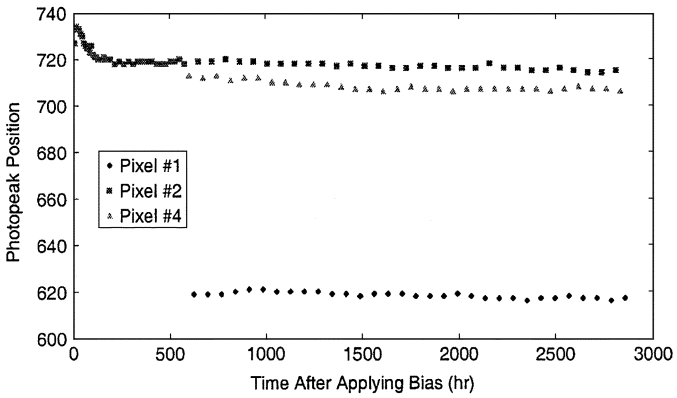

Fig. 16. Peak position for the three working pixels does not vary much after the first few days once the bias is applied.

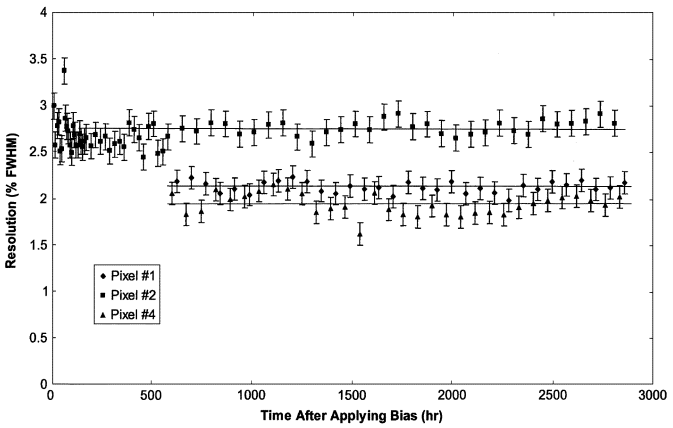

Fig. 17. Depth corrected resolution as a function of time after biasing the detector. The straight lines depict the average depth corrected resolution. Most daily resolution measurements were within the 0.1% FWHM error of the measurement.

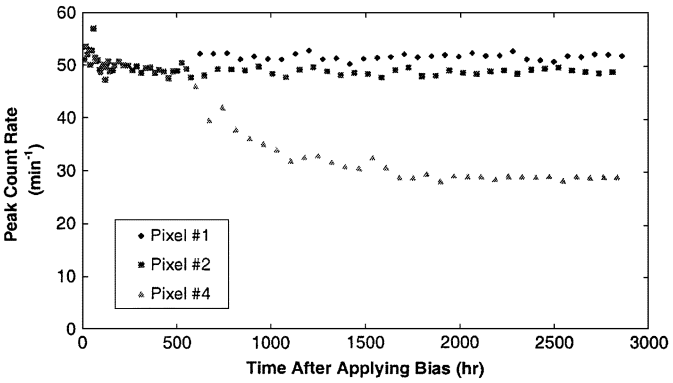

Fig. 18. While the peak count rate remains relatively constant for pixels #1 and #2, pixel #4 shows a decreasing count rate with time, suggesting that the effective volume of the pixel decreased by approximately 35%. Material nonuniformity and space effects may be caused this decrease.

constant. The results from the first four days of measurements showed that the peak information remained relatively consistent and suggest that little, if any, polarization occurred during the first 3–4 days after biasing the detector. This result is contrary to the results previously presented by others using planar electrodes. Improvements in the growth of HgI_2 material used in the pixelated detectors may have contributed in the reduction of polarization effects.

VI. Long-Term Stability of HgI_2

In addition to collecting spectra over the first week, spectra were obtained over a several month period in order to observe any long term changes in gamma-ray spectra obtain from pixelated HgI_2 detectors. After 25 days of measuring only pixel #2, alternating measurements including pixels #1 and #4 were made to observe any long term polarization effects on the other working pixels. Fig. 16 shows the overall photopeak position as a function of time after biasing. The overall peak position on all three pixels remained relatively constant over the nearly 4 months of operation. Aside from the decrease on pixel #2 during the first few days of operation, the peak position on all three pixels varied by no more than 10 channels on any pixel, or about 1.5%. A line was fit to the peak position information for each pixel and showed that, at worst, the peak position decreased by 1 channel every 15.4±0.3 days. Each pixel had its own independent counting chain and the difference in the peak positions between pixels can be accounted for by differences in the capacitance of the pre-amplifier.

The depth corrected resolution (Fig. 17) also remained consistent over the course of operation. Pixel #2's resolution remained near 2.8%, while the other two pixels had depth corrected resolution near 2%, with pixel #4 average about 1.9% FWHM. While the resolution appears to be erratic and shows much variation, the error in the calculation of the FWHM is about one channel, which corresponds to ±0.1%.

The photopeak count rate of pixel #4 showed a significant decrease over time (Fig. 18) of about 35%. The results suggest that the effective volume of this pixel (the volume that will contribute peak counts to the pixel spectra) is decreasing, while the other two pixels remain constant. This may have been caused by the accumulation of space charge in the gap region between the pixel and the surrounding large anode. The accumulation of space charge may have caused a change in the electric field in the gap region, which could cause the effective volume of the pixel to decrease. In addition, pixel #4 is adjacent to pixel #3, and this pixel did not have a signal, suggesting the electrode was not in contact with the detector crystal. This decrease can also be observed on pixel #2 (also adjacent to the bad pixel). However the effect was not as severe as pixel #4, with a decrease in peak count rate of only 0.9% (slightly above the measurement error of ∼0.6%) from 500 to 2500 h after application of bias. Significant material nonuniformity (such as a larger concentration of impurities) may have caused a larger accumulation of space charge within pixel #4 when compared with other pixels.

VII. Testing the Augur Recombination Model

One advantage of the pixelated HgI_2 detectors is that models for trapping and charge transport can be tested and evaluated [16]. Polarization models can also be tested for their validity. The polarization model proposed by Gerrish [10] suggests that auger recombination is a major component. This is a process in which a hole recombines with an electron trapped in a multiple-electron trap site. The energy that is released in the recombination process can lead to the release of another electron into the conduction band was tested using pixelated HgI_2. The auger

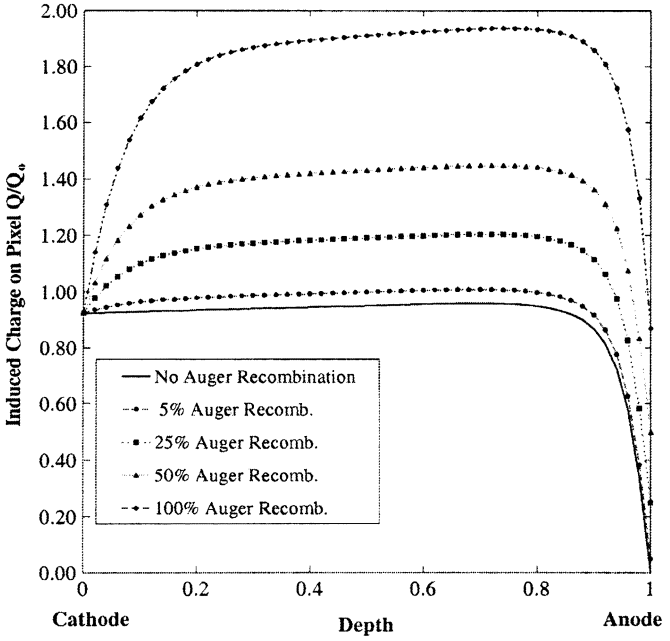

Fig. 19. Effect of Auger recombination should cause a very large pulse shift over a large portion of the pixel volume. However, only a small shift was observed, suggesting that Auger recombination has little effect on polarization is current pixelated HgI_2 detectors.

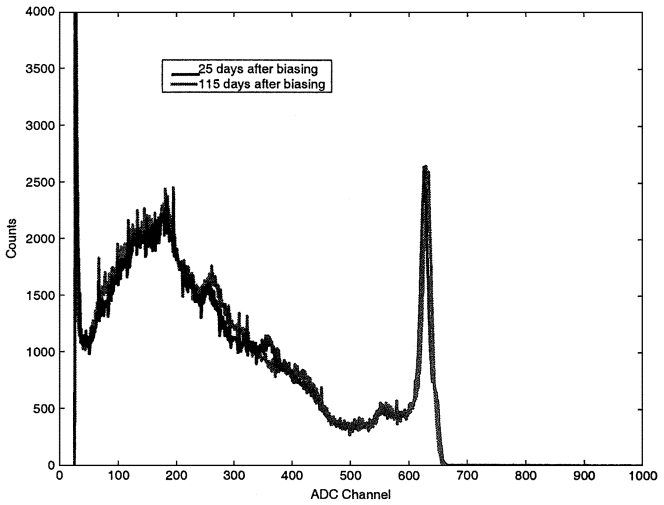

Fig. 20. Cs-137 spectra from pixel #1 on the first day it was measured (25 days after biasing) and 3 months later. Note that there was very little change in the spectra, demonstrating that current pixelated HgI_2 detectors can be stable over several months of operation.

recombination can result in two electrons being collected for each electron-hole pair created in an interaction event, and the amount of recombination should decrease over time. Thus, there would be a large shift in the gamma-ray spectrum to lower energies over a period of several weeks.

Since the number of collected electrons mainly determines the signal generated on an anode pixel, induced charge on the pixel can be significantly affected by the amount of auger recombination in the detector. Fig. 19 shows how the induced charge on the pixel would be affected by different amounts of auger recombination. The induced charge on the pixel would nearly double if the auger recombination was the main process associated with hole trapping. As auger recombination slowly reduces, the induced charge on the pixel will decrease. Subsequently, a large shift in the photopeak position should be observed. However, that was not the case with the current pixelated HgI_2 detectors, as the photopeak shift was only of the order of a few percent or less over several months (Fig. 16) for any measured pixel. In fact, very little change can be observed from the gamma-ray spectra (see Fig. 20). Thus, either auger recombination was not a valid polarization model, or the process is very minor. This small of peak shift may also be attributed by the loss of electron collection from the anode pixel. This may be from a buildup of space charge in the detector, particularly in the gap region where the electric field may be weak leading to increase electron trapping. An improvement in detector crystal growth and fabrication may have also kept polarization effects to a minimum in the current detector.

VIII. Summary and Conclusions

Pixelated HgI_2 detectors have shown ability to produce spectra with energy resolutions less than 2% FWHM from individual pixels for the Cs-137 662 keV gamma-ray. These detectors can be operated at room temperature with modest electric fields and shorter shaping times than similar detector using conventional planar electrodes. Unlike thick conventional electrode HgI_2 detectors, pixelated HgI_2 can provide good spectral results from the full thickness of the detector since only electron collection is needed to produce the full pulse amplitude. As a precursor to designing a fully pixelated HgI_2 detector, the new layout placed all four pixels in the center region of the detector. While the results with the new detectors were mostly positive, the resolution of these detectors was worse than expected. This was due to the large gap between the pixels and the surrounding large anode and the bad pixel. This large gap caused more charge sharing between the anodes, which in turn degraded the resolution by increasing the low energy tailing on the photopeak. In addition, the number of events in the Compton continuum increased dramatically due to increased charge sharing over the anode electrode design.

After a small amount of polarization (observed as a shift in the photopeak position) during the first four days the detector was under bias, 2 of 3 measured pixels on the HgI_2 detector performed well over several months of continual operation. The peak position and resolution remained relatively constant for all three pixels that were measured. One pixel (pixel #4) suffered from a reduced photopeak count rate with time, suggesting the effective volume of the pixel was changing. This pixel may have suffered from a significant amount of material defects and space charge buildup resulting in a loss of effective volume when compared with the other working pixels. The other two pixel each had a count rate that remained relatively stable throughout the measurement period.

One aspect of pixelated HgI_2 detectors is that through the use of depth sensing and single polarity charge sensing, many characteristics of the detector physics can be studied, including models of charge transport, charge trapping, and polarization. In this paper, a previously proposed model for polarization, Auger recombination, has been evaluated and shown not to be an issue

for current pixelated HgI_2 detectors. In fact, polarization was, at most, a small factor that can be accounted for in pixelated HgI_2.

Several improvements in the detector design need to be incorporated before proceeding to build a fully pixelated HgI_2 detector. The gap between pixel electrodes needs to be reduced. Reducing the gap will reduce the number of interactions in the gap region and subsequently decrease the amount of charge sharing. The Compton continuum will be reduced and the resolution of photopeaks should improved from a reduction of low energy tailing. Multiple pixel readout should also be incorporated into the HgI_2 detector system. Multiple pixel readout will allow for the reconstruction of both multiple scatter events that deposit the full gamma-ray energy in the detector, and to correct charge sharing events from adjacent pixels. Multiple pixel readout will increase the overall photopeak efficiency of pixelated HgI_2 detectors.

REFERENCES

[1] W. R. Willig, "Mercury iodide as a gamma spectrometer," *Nucl. Instrum. Methods*, vol. 96, pp. 615–616, Nov. 1971.

[2] K. Hull, A. Beyerle, B. Lopez, J. Markakis, C. Ortale, W. Schnepple, and L. van den Berg, "Recent developments in thick mercuric iodide spectrometers," *IEEE Trans. Nucl. Sci.*, vol. 31, pp. 402–404, Feb. 1983.

[3] P. Olmos, G. Garcia-Belmonte, J. M. Perez, and J. C. Diaz, "Use of thick HgI_2 detectors as intelligent spectrometers," *Nucl. Instrum. Methods*, vol. A299, pp. 45–50, Dec. 1990.

[4] V. M. Gerrish, D. J. Williams, and A. G. Beyerle, "Pulse filtering for thick mercuric iodide detectors," *IEEE Trans. Nucl. Sci.*, vol. 34, pp. 85–90, Feb. 1987.

[5] H. H. Barrett, J. D. Eskin, and H. B. Barber, "Charge transport in arrays of semiconductor gamma-ray detectors," *Phys. Rev. Lett.*, vol. 75, pp. 156–160, July 1995.

[6] J. E. Baciak and Z. He, "Spectroscopy on thick HgI_2 detectors: A comparison between planar and pixelated electrodes," *IEEE Trans. Nucl. Sci.*, vol. 4, pp. 1220–1224, Aug. 2003.

[7] ——, "Comparison of 5-mm and 10-mm-thick HgI_2 pixelated γ-ray spectrometers," *Nucl. Instrum. Methods*, vol. A505, pp. 191–194, June 2003.

[8] R. O. Bell, G. Entine, and H. B. Serreze, "Time-dependent polarization of CdTe gamma-ray detectors," *Nucl. Instrum. Methods*, vol. 117, pp. 267–271, 1974.

[9] A. Holzer and M. Schieber, "Reduction of polarization in mercuric iodide nuclear radiation detectors," *IEEE Trans. Nucl. Sci.*, vol. 27, pp. 266–271, Feb. 1980.

[10] V. Gerrish, "Polarization and gain in mercuric iodide gamma-ray spectrometers," *Nucl. Instrum. Methods*, vol. A322, pp. 402–413, Feb. 1992.

[11] J. E. Baciak, Z. He, and R. P. DeVito, "Electron trapping variations in single-crystal pixelated HgI_2 gamma-ray spectrometers," *IEEE Trans. Nucl. Sci.*, vol. 59, pp. 1264–1269, June 2002.

[12] Z. He, G. F. Knoll, D. K. Wehe, R. Rojeski, C. H. Mastrangelo, M. Hammig, C. Barrett, and A. Uritani, "1-D position sensitive single carrier semiconductor detectors," *Nucl. Instrum. Methods*, vol. A380, pp. 228–231, Oct. 1996.

[13] Amptek, Inc., 6 De Angelo Drive, Bedford, MA 01730, USA.

[14] National Instruments Corporation, 11500 North Mopac Expressway, Austin, TX 78759. .

[15] W. Li, Z. He, G. F. Knoll, D. K. Wehe, and J. E. Berry, "Spatial variation of energy resolution in 3-D position sensitive CZT gamam-ray spectrometers," *IEEE Trans. Nucl. Sci.*, vol. 46, pp. 187–192, June 1999.

[16] J. E. Baciak and Z. He, "Development of a model for gamma-ray spectra generation using pixelated mercuric iodide detectors," in *Proc. SPIE*, vol. 4784, 2002, pp. 119–127.